THE JOURNAL OF BIOLOGICAL CHEMISTRY
Vol. 272, No. 33, Issue of August 15, pp. 20443–20450, 1997
Printed in U.S.A.
© 1997 by The American Society for Biochemistry and Molecular Biology, Inc.

Gelsolin Binding to Phosphatidylinositol 4,5-Bisphosphate Is Modulated by Calcium and pH*

(Received for publication, April 24, 1997, and in revised form, May 22, 1997)

Keng-Mean Lin‡, Elizabeth Wenegieme‡, Pei-Jung Lu§, Ching-Shih Chen§, and Helen L. Yin‡¶

From the ‡Department of Physiology, University of Texas Southwestern Medical Center, Dallas, Texas and the §Division of Medicinal Chemistry and Pharmaceutics, College of Pharmacy, University of Kentucky, Lexington, Kentucky 40536-0082

The actin cytoskeleton of nonmuscle cells undergoes extensive remodeling during agonist stimulation. Lamellipodial extension is initiated by uncapping of actin nuclei at the cortical cytoplasm to allow filament elongation. Many actin filament capping proteins are regulated by phosphatidylinositol 4,5-bisphosphate (PIP_2), which is hydrolyzed by phospholipase C. It is hypothesized that PIP_2 dissociates capping proteins from filament ends to promote actin assembly. However, since actin polymerization often occurs at a time when PIP_2 concentration is decreased rather than increased, capping protein interactions with PIP_2 may not be regulated solely by the bulk PIP_2 concentration. We present evidence that PIP_2 binding to the gelsolin family of capping proteins is enhanced by Ca^{2+}. Binding was examined by equilibrium and nonequilibrium gel filtration and by monitoring intrinsic tryptophan fluorescence. Gelsolin and CapG affinity for PIP_2 were increased 8- and 4-fold, respectively, by μM Ca^{2+}, and the Ca^{2+} requirement was reduced by lowering the pH from 7.5 to 7.0. Studies with the NH_2- and COOH-terminal halves of gelsolin showed that PIP_2 binding occurred primarily at the NH_2-terminal half, and Ca^{2+} exposed its PIP_2 binding sites through a change in the COOH-terminal half. Mild acidification promotes PIP_2 binding by directly affecting the NH_2-terminal sites. Our findings can explain increased PIP_2-induced uncapping even as the PIP_2 concentration drops during cell activation. The change in gelsolin family PIP_2 binding affinity during cell activation can impact divergent PIP_2-dependent processes by altering PIP_2 availability. Cross-talk between these proteins provides a multilayered mechanism for positive and negative modulation of signal transduction from the plasma membrane to the cytoskeleton.

Phosphoinositides are important in signal transduction, both as precursors to signaling molecules and as physical anchors and regulators of proteins (1, 2). Among these, the D4 phosphoinositide, phosphatidylinositol 4,5-bisphosphate (PIP_2),[1] has been implicated as a potential mediator of actin cytoskeletal rearrangements (3, 4). PIP_2 modulates many actin regulatory proteins. These include the following: actin severing and/or capping proteins (gelsolin (5), CapG (6), and capping protein (also known as Cap Z) (7)), monomer-binding proteins (profilin (8) and cofilin (9)), and other actin-binding proteins (α-actinin (10) and vinculin (11)). It has been hypothesized that PIP_2 induces explosive actin assembly by dissociating capping proteins from filament ends and releasing actin monomers from actin-sequestering proteins (3, 7, 12). The involvement of PIP_2 in actin polymerization is supported by recent experiments that show that Rac1 and RhoA, monomeric GTPases of the Rho family that have well defined effects on the cytoskeleton (13), stimulate the synthesis of PIP_2 (14–16). Furthermore, manipulations that alter the availability of PIP_2 in cells have profound effects on agonist and/or Rac1-induced filament end capping, actin polymerization, and cell motility (16, 17). However, although the time courses of PIP_2 hydrolysis and recovery correlate in some cells (16, 18), they do not in most of the cells examined (19–21). Particularly puzzling is the finding that, in many cells, actin polymerizes at a time when PIP_2 level is reduced, rather than increased, as would be expected if uncapping and monomer desequestration are initiated by PIP_2. To explain this discrepancy, it is often hypothesized that local PIP_2 availability can be enhanced by compartmentalization or differential turnover (22–24), even as the bulk PIP_2 mass is reduced. The equally attractive possibility that PIP_2 binding is regulated by signals generated during agonist stimulation has not been considered.

Agonist-stimulated cells exhibit complex Ca^{2+} oscillations and pH transients. These signals alter the binding of gelsolin and CapG to actin, by inducing a conformational change (6, 25–27). In this study, we tested the effect of Ca^{2+} and pH on the binding of the gelsolin family proteins to PIP_2 and found that they affect PIP_2 binding in an interdependent manner. We identified the domains in gelsolin that impart such regulation and elucidated the relation between the NH_2-terminal and COOH-terminal halves of the protein. Since gelsolin modulates the activity of many PIP_2-regulated proteins with important signaling functions *in vivo* (28) and *in vitro* (29–31), our results have important implications for how the gelsolin family proteins are regulated during agonist signaling and how the activity of other PIP_2-dependent cytoskeletal and noncytoskeletal proteins can be coordinated.

EXPERIMENTAL PROCEDURES

Expression and Purification of Recombinant CapG, Gelsolin, and Gelsolin Domains—Gelsolin has six semihomologous domains (S1–6), which can be further divided into two functional halves (32). The expression vectors for the gelsolin NH_2-terminal half (S1–3), gelsolin S1, gelsolin S2–3, and CapG have been described previously (33–35). The full-length gelsolin expression vector (encompassing the entire human plasma gelsolin coding sequence) was constructed by ligating gelsolin cDNA to *pet3a* via the *Bam*HI site. Recombinant proteins were expressed in bacteria and purified using sequential anion and cation

* This work was supported by National Institutes of Health Grants RO1 GM5112 (to H. L. Y.) and GM53448 (to C. S. C.) and individual National Research Service Award GM17997 (to E. W.). The costs of publication of this article were defrayed in part by the payment of page charges. This article must therefore be hereby marked "*advertisement*" in accordance with 18 U.S.C. Section 1734 solely to indicate this fact.

¶ To whom correspondence should be addressed: Dept. of Physiology, U.T. Southwestern Medical Center at Dallas, 5323 Harry Hines Blvd., Dallas, TX 75235-9040. Tel.: 214-648-7967; Fax: 214-648-8685; E-mail: yin01@utsw.swmed.edu.

[1] The abbreviation used is: PIP_2, phosphatidylinositol 4,5-bisphosphate.

This is an Open Access article under the CC BY license.

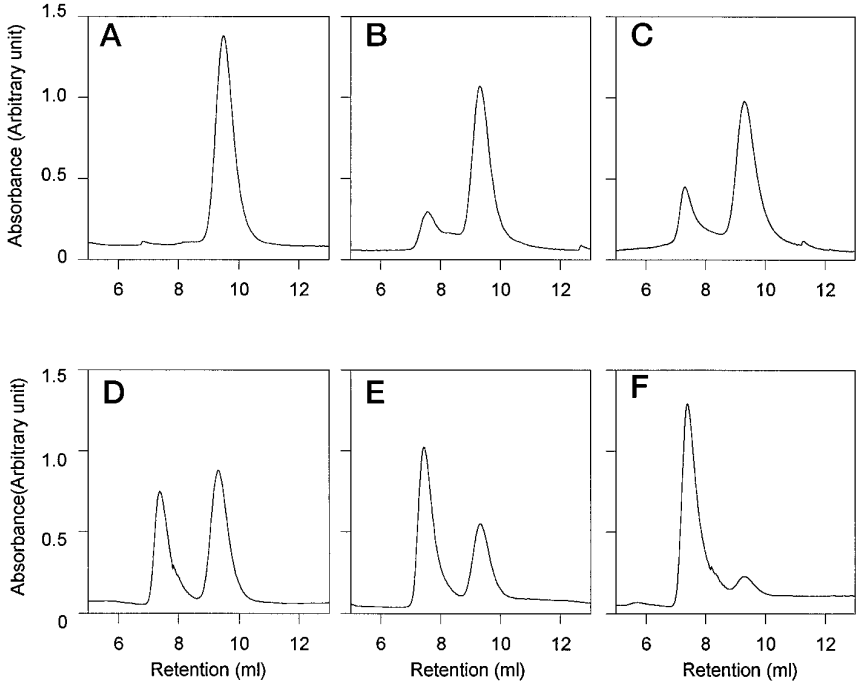

FIG. 1. **Small zone gel filtration of CapG.** *A–F*, elution profiles of CapG with increasing PIP_2 concentration. CapG (5.5 μM) was incubated with PIP_2 micelles in a pH 7.5 buffer containing 0.4 mM EGTA. PIP_2 concentrations were 0, 14.2, 22.7, 28.3, 56.7, and 113.3 μM for *A–F*, respectively.

exchange chromatography (34). Protein concentration was determined by the method of Bradford (36), and protein purity was assessed by SDS-polyacrylamide gel electrophoresis.

The COOH-terminal half expression vector was constructed by using polymerase chain reaction to generate a fragment encompassing human plasma gelsolin nucleotides 1298–1753. The forward primer contains a *Xho*I site (ACC TCC ACT CTC GAG GCC GCC), and the reverse primer has a *Sma*I site (CAA CAG CCC GGG TGG CT). The polymerase chain reaction product was cloned into Bluescript KS+ via the *Xho*I/*Sma*I sites. This construct was digested with *Sma*I and blunt end-ligated with a downstream gelsolin fragment. The fragment was excised with *Bam*HI from full-length gelsolin cDNA in Bluescript KS+ (gelsolin *Sma*I site at nucleotide 1750 and vector multiple cloning *Sma*I site downstream of the termination codon). The resultant cDNA was digested with *Spe*I (in the 3′ multiple cloning region, downstream of *Sma*I) and filled in with CT nucleotides to create a site with a two-base overhang compatible with that of *Hin*dIII. The other end was released by digestion with *Xho*I and ligated to PGEX K6 vector that was linearized with *Hin*dIII (site partially filled in with nucleotides AG to generate a two-base overhang compatible with the partially filled in *Spe*I) and *Xho*I. The fusion protein contained a 30-kDa GST followed by a 40-kDa gelsolin COOH-terminal half. The COOH-terminal gelsolin was cleaved from GST bound to a column with thrombin.

Phospholipid—PIP_2 was purchased from Calbiochem. Micelles were prepared by dissolving the dried lipid in water to a final concentration of 2 mg/ml and sonicating for 5 min. at maximum power (model W185; Heat Systems Ultrasonics, Inc., Farmingdale, NY). Large unilamellar vesicles at a 5:1 phosphatidylcholine:PIP_2 ratio were made with an extruder (Lipex Biomembranes, Vancouver, Canada) as described by Machesky *et al.* (37).

Small Zone Gel Filtration—The assay was similar to that described previously for studying lipid binding to most actin regulatory proteins (33, 35, 38). This is because small proteins bound to PIP_2 micelles or mixed vesicles migrate faster than the unbound proteins. Proteins were incubated with lipid for 30 min at room temperature, and 100 μl of the mixture was chromatographed at 4 °C through a Superdex 75 HR 10/30 column (Pharmacia Biotech Inc.), equilibrated with pH 7.0 or 7.5 buffers containing 25 mM Hepes, 100 mM KCl, 0.5 mM β-mercaptoethanol, 0.4 mM EGTA with or without $CaCl_2$. Lipid was not included in the elution buffer. Fractions were eluted at 0.5 ml/min, and 0.5-ml fractions were collected. The elution profile was monitored by absorbance at 280 nm. The amount of unbound protein was determined from the protein absorbance peak. The lipid-bound protein was calculated as the difference between the total protein applied minus the unbound protein. The apparent dissociation constant (K_d) was calculated as follows.

$$K_d = [\text{protein}]_{\text{free}} \times [\text{lipid}]_{\text{free}}/[\text{protein-lipid}] \qquad \text{(Eq. 1)}$$

Equilibrium Gel Filtration—The method of Hummel and Dreyer (39), as modified by Machesky *et al.* (37) was used. A Superose 12 HR 10/30 column (Pharmacia) was equilibrated with CapG (ligand) in a buffer containing 25 mM Hepes, 75 mM KCl, 0.5 mM dithiothreitol, 1.8 mM NaN_3, 0.05 μM $CaCl_2$, pH 7.5, at room temperature. 100 μl of the equilibration buffer containing CapG was incubated with PIP_2 micelles for 30 min and loaded onto the column. The column was developed with the equilibration buffer containing CapG at 0.25 ml/min, and 0.3-ml fractions were collected. CapG concentration in the column fractions was monitored by UV absorption. The amount of CapG bound to PIP_2 was determined from the trough in the absorbance peak. Multiple runs using equilibration CapG concentrations of 0.96, 1.3, 2.6, and 3.9 μM and PIP_2 concentrations of 34, 46, 68, and 91 μM were done. K_d was determined by the equation,

$$r = \frac{B_{\max}[\text{protein}]_{\text{free}}}{K_d + [\text{protein}]_{\text{free}}} \qquad \text{(Eq. 2)}$$

where r is the ratio of protein bound to each PIP_2 molecule at a given PIP_2 concentration and $B_{\max}$ is the maximum number of protein bound per PIP_2 at saturation.

Quenching of Intrinsic Tryptophan Fluorescence—Fluorescence spectra were recorded at 30 °C with a QM-1 fluorometer (Photon Technology International, Canada). 2 ml of a protein solution (0.3 μM, 30 °C) in 25 mM Hepes, 100 mM KCl, 0.4 mM EGTA, 0.5 mM β-mercaptoethanol, pH 7.5, with or without 36 μM free Ca^{2+} were placed in a 1-cm square quartz cuvette and stirred with a minimagnetic stirrer. After allowing 5 min for equilibration, the tryptophan fluorescence spectrum was recorded by excitation at 292 nm. The excitation and emission beam slits were set at 3 and 2 nm bandwidth, respectively. PIP_2 micelles (at final PIP_2 concentrations ranging from 0.042 to 32.3 μM, depending on the protein studied) were added at 2-μl increments, and the fluorescence spectra were recorded 5 min after each addition. The total volume of micelles added did not exceed 2% of the initial protein solution volume. The decrease in fluorescence emission at 320 nm was plotted as a function of PIP_2 concentration, and the fluorescence change was assumed to be proportional to the concentration of the protein-phosphoinositide complex. Data were analyzed as described by Ward (40). The apparent dissociation constant, K_d, was calculated using the equation,

$$\Delta F = (\Delta F_{\max} \times [\text{lipid}_T])/(K_d + [\text{lipid}_T]) \qquad \text{(Eq. 3)}$$

where ΔF is the fluorescence quenching at a given PIP_2 concentration, $\Delta F_{\max}$ is the total fluorescence quenching of the protein saturated with ligand, and $[\text{lipid}_T]$ is the concentration of PIP_2. $\Delta F_{\max}$ is estimated by curve fitting of the binding data using the Hyperbol.fit program in

TABLE I
Binding of CapG to PIP_2

K_d for fluorescence titration was calculated using Equation 4. K_d values for gel filtration data were calculated with Equation 1, assuming a stoichiometry of 2. Values shown are mean ± S.E., determined at pH 7.5.

K_d (μM)						
Fluorescence				Gel filtration		
				Small zone		
EGTA	Ca^{2+}	p^a	h^b	EGTA	Ca^{2+}	Equilibrium (Ca^{2+})
24.4 ± 5.9 (n = 3)[c]	6.0 ± 0.8 (n = 3)	1.7	1.1 ± 0.03 (n = 3)	69.0 ± 5.3 (n = 5)	29.4 ± 2.5 (n = 7)	7.0 ± 0.5 (n = 5)

[a] p, mol of PIP_2/mol of CapG, average of two determinations.
[b] h, Hill coefficient.
[c] n, number of independent experiments.

SigmaPlot. Alternatively, the intrinsic association constant (K_a) as well as the stoichiometry of binding (p) can be derived using the graphical method of Stinson and Holbrook (41),

$$\frac{1}{(1-\theta)K_a} = \frac{[\text{lipid}_T]}{\theta} - p[\text{protein}_T] \qquad \text{(Eq. 4)}$$

where θ is the fractional binding ($\Delta F/\Delta F_{max}$), p is the stoichiometry of binding, [lipid_T] is the total concentration of PIP_2, and [protein_T] is the total acceptor concentration. When $1/(1-\theta)$ is plotted against lipid_T/θ, a straight line with a slope of K_a and an intercept of $\text{protein}_T/\theta$ is obtained. The stoichiometry of interaction (p) can be calculated by dividing the intercept with the protein concentration.

Measurement of Free Ca^{2+} Concentration and pH—The concentrations of free Ca^{2+} in EGTA containing solutions with varying amounts of Ca^{2+} were measured with Ca^{2+}-sensitive dyes. 5 μM Fura-2 was used to determine Ca^{2+} concentrations below 1 μM. Free Ca^{2+} concentration was calculated (26) assuming the K_d of the Fura-2-Ca^{2+} complex is 229 nM at pH 7.0 and 144 nM at pH 7.5. Calcium green 5N (Molecular Probes, Eugene, OR) was used to measure Ca^{2+} concentrations higher than 1 μM, and free Ca^{2+} concentration was calculated assuming a K_d of 14 μM.

RESULTS

CapG Binding to PIP_2—Small zone gel filtration analyses showed that CapG bound to PIP_2 micelles in a dose-dependent manner. Micelle-bound CapG eluted in the void volume that was well separated from the free protein peak (Fig. 1). Binding to phosphatidylcholine-PIP_2 vesicles gave similar results (data not shown), suggesting that micelles could be used to assess binding, although it is not a physiological substrate. To facilitate comparison under different binding conditions and between different proteins, we attempted to calculate a K_d. Equilibrium binding studies suggest that each CapG binds two PIP_2 molecules (see below). Assuming this stoichiometry, the apparent K_d for binding to PIP_2 micelles (calculated using Equation 1) was 69.0 μM in 1 mM EGTA, and 29.4 μM in the presence of 36 μM Ca^{2+} at pH 7.5 (Table I). These values represent the upper limit, since measurements were not made under equilibrium conditions.

To determine if there is indeed a Ca^{2+}-induced change, equilibrium binding studies based on the quenching of CapG intrinsic tryptophan fluorescence by PIP_2 were performed. This method has been used to study the binding of profilin (43), phospholipase Cδ (44), and dynamin pleckstrin homology domain (45) to PIP_2. CapG had an emission maximum of 327 nm, and 36 μM Ca^{2+} produced a small reduction in fluorescence intensity (the ratio of peak fluorescence in EGTA/Ca^{2+} is 0.92 ± 0.05 (mean ± S.E., n = 5) (Fig. 2, *A* and *B*). PIP_2 induced a dose-dependent and saturable decrease in intrinsic fluorescence, without shifting the emission maximum. Micelles alone without CapG did not have significant emission (data not shown). A plot of CapG fluorescence quenching *versus* PIP_2 concentration showed that saturation was reached at a lower PIP_2 concentration in the presence of Ca^{2+} than in EGTA (Fig. 3*A*). The K_d values for binding at pH 7.5, calculated according to Equation 3, were 31.9 and 8.4 μM in EGTA and Ca^{2+},

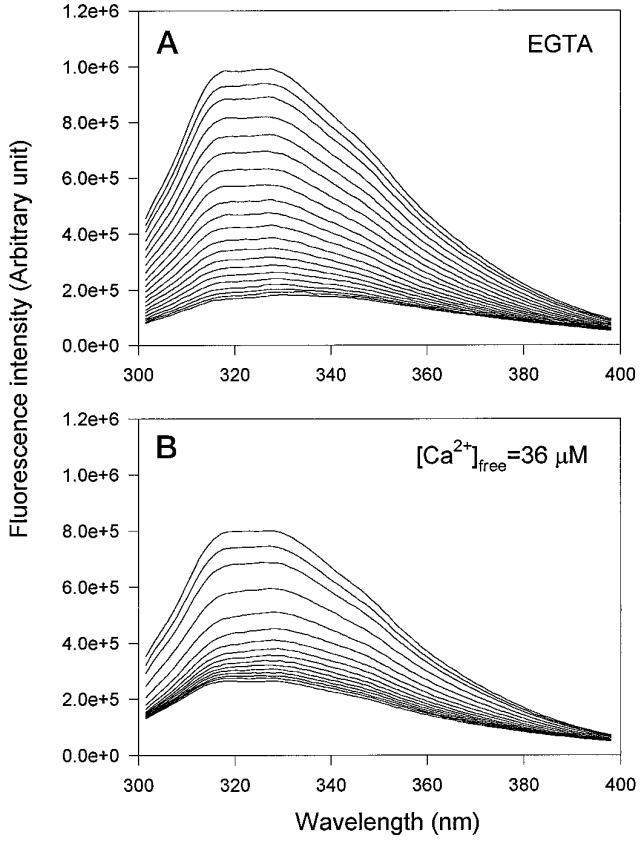

FIG. 2. **Tryptophan fluorescence emission spectra of CapG.** 2 μl of 0.85 mM PIP_2 micelles were added sequentially to CapG in the absence or presence of 36 μM free Ca^{2+}. *A*, emission curves of 0.3 μM CapG in a pH 7.5 buffer in the presence of 0.4 mM EGTA. The *top curve* was without PIP_2, and the remaining curves were with PIP_2 ranging from 0.85 to 32.3 μM. *B*, emission curves in the presence of 36 μM free Ca^{2+} and 0–32 μM PIP_2, as described in *A*.

respectively, for the experiment shown. Similar values (24.4 and 6.0 μM) were obtained when the data were analyzed using Equation 4 (Table I). These K_d values were 3–4 times lower than the small zone gel filtration values, suggesting that CapG-PIP_2 complexes dissociate during nonequilibrium gel filtration. Using a similar protocol, human platelet profilin binds PIP_2 with a K_d of 35 μM (43), and binding is not affected by Ca^{2+}.

The stoichiometry of CapG binding was 1.7 in either Ca^{2+} or EGTA (Table I). Since CapG has one known PIP_2 binding site (6, 33), this site appears to bind two PIP_2 molecules. The two PIP_2 bound independently and noncooperatively, as indicated by the Hill coefficients of close to 1 (1.02 ± 0.05 and 1.09 ± 0.02 in EGTA and Ca^{2+}, respectively) (Fig. 3*B*, Table I). The exact meaning of this stoichiometry is not clear, because each micelle contains multiple PIP_2 and CapG can potentially bind more than one micelle. Nevertheless, the calculated stoichiometry is

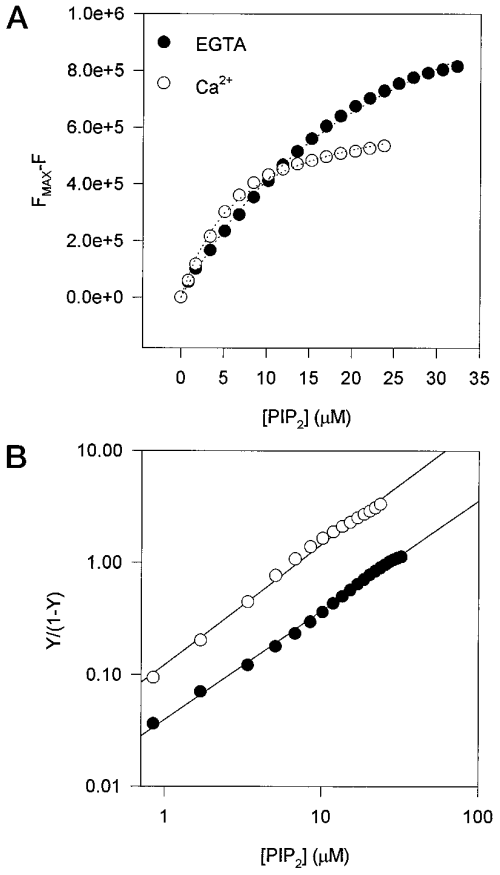

FIG. 3. **Analysis of CapG fluorescence titration data.** *A*, binding curves plotting ($F_{max} - F$) *versus* PIP_2 concentration. *Closed* and *open circles* represent experimental points in 0.4 mM EGTA or 36 μM Ca^{2+}. *Dotted lines* are fitted to the experimental points, and F_{max} values were obtained. K_d values with and without Ca^{2+} were 8.4 and 31.9 μM, respectively, for this experiment. *B*, Hill plot of the titration data. The Hill equation is rearranged and plotted to show the relation between the log(Y/(1 − Y)) and log[lipid$_T$], where Y is the fractional saturation. h, the Hill coefficient, is derived from the slope (1.1 and 0.97 in the presence of Ca^{2+} and EGTA for this experiment).

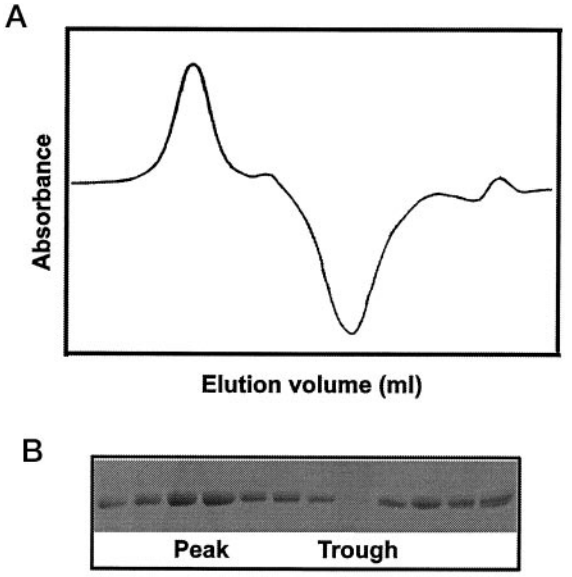

FIG. 4. **Hummel-Dyer equilibrium gel filtration to characterize CapG binding to PIP$_2$ micelles.** *A*, elution profile. The column was equilibrated with 1.4 μM CapG, and 68 μM CapG was added. *B*, Coomassie Blue staining of CapG in column fractions. 50-μl aliquots were lyophilized and analyzed by SDS-polyacrylamide gel electrophoresis.

useful for comparison among different proteins.

Equilibrium gel filtration validated the K_d derived by fluorescence titration. The column was preequilibrated with CapG, and PIP_2 incubated with CapG in the equilibrating buffer was added. The column was then developed with CapG containing equilibration buffer. CapG bound to PIP_2 migrated faster, increasing the CapG content above the equilibration level (peak) and depleting the amount in the trailing fractions (trough) (Fig. 4, *A* and *B*). Assuming that each CapG bound two PIP_2 molecules (see Table I), the K_d obtained from five experiments performed with a range of CapG and/or PIP_2 concentration was 8.1 ± 0.9 μM (mean ± S.E.). This is comparable with the spectroscopic titration result, affirming the validity of the two independent methods.

Gelsolin Binding to PIP$_2$—Tryptophan titration could not be used to study gelsolin binding to PIP_2 because the full-length gelsolin signal (without phosphoinositide) fluctuated and did not reach a steady level even after 20 min. The reason for this instability was not investigated further. Gel filtration experiments showed that gelsolin binding to PIP_2 was enhanced by Ca^{2+} (Fig. 5, *A–F*). At pH 7.5, the apparent K_d values were 305.4 and 40.2 μM with and without Ca^{2+} (Table II). The latter value is similar to that of CapG, indicating that gelsolin and CapG have comparable PIP_2 binding affinity in the presence of Ca^{2+}. However, in EGTA, gelsolin has a much higher K_d than CapG, suggesting that Ca^{2+} induces a larger change in binding affinity. This could be due to a disproportionate increase in k_{off} relative to k_{on}. 10 μM Mg^{2+} did not substitute for Ca^{2+} (data not shown), consistent with previous results (46).

The effect of Ca^{2+} was amplified when the pH was shifted from 7.5 to 7.0 (Fig. 5, compare *A–C* with *D–F*). The relations among K_d, Ca^{2+}, and pH are shown in Fig. 5*G*. In the absence of Ca^{2+}, decreasing pH from 7.5 to 7.0 had minimal effect (K_d of 300 and 350 μM, respectively). This is not surprising, since PIP_2 protonation is not expected to change substantially within this narrow pH range (47) and a broader pH range does not affect binding of profilin to PIP_2 either (37). However, at pH 7.0, less Ca^{2+} was required to increase binding. 0.2 μM Ca^{2+} decreased the K_d by half at pH 7.0, while 4.5 μM Ca^{2+} was required to produce the same effect at pH 7.5. Both Ca^{2+} concentrations are well within the range achieved following agonist stimulation, particularly at the cytoplasm immediately subjacent to the plasma membrane.

Ca^{2+} and pH Regulation of Gelsolin Domains—To determine which part of gelsolin contributes to the Ca^{2+} and/or pH dependence of PIP_2 binding, we examined the PIP_2-binding characteristics of several gelsolin domains. Gelsolin contains six segmental repeats, S1–6 (32). The NH_2-terminal half encompassing S1–3 binds actin independently of Ca^{2+} (48) and has two known PIP_2 binding sites and potentially a third unmapped site (33, 49, 50). The COOH-terminal half (S4–6), which requires Ca^{2+} to bind actin (51), has not been examined previously for PIP_2 binding.

Unlike full-length gelsolin, the gelsolin NH_2-terminal half behaved well during fluorescence titration (Fig. 6*A*). It bound PIP_2 with high affinity, and saturation was reached at a slightly lower PIP_2 concentration in EGTA than in Ca^{2+} (the opposite of full-length gelsolin and CapG). The K_d values for the experiment shown in Fig. 6*A* were 1.2 and 2.9 μM, respectively. The stoichiometry of binding, derived from Fig. 6*B*, was 3.4. This value is twice that of CapG, confirming that gelsolin NH_2-terminal half has more PIP_2 binding sites (33). Gel filtration studies confirmed that Ca^{2+} increased the K_d. The Hill coefficient of 1.1 ± 0.03 (Fig. 6*C*, Table II) suggested that binding was noncooperative and that the sites bound PIP_2-independently. S1, which has one PIP_2 site, bound 1.6 mol of

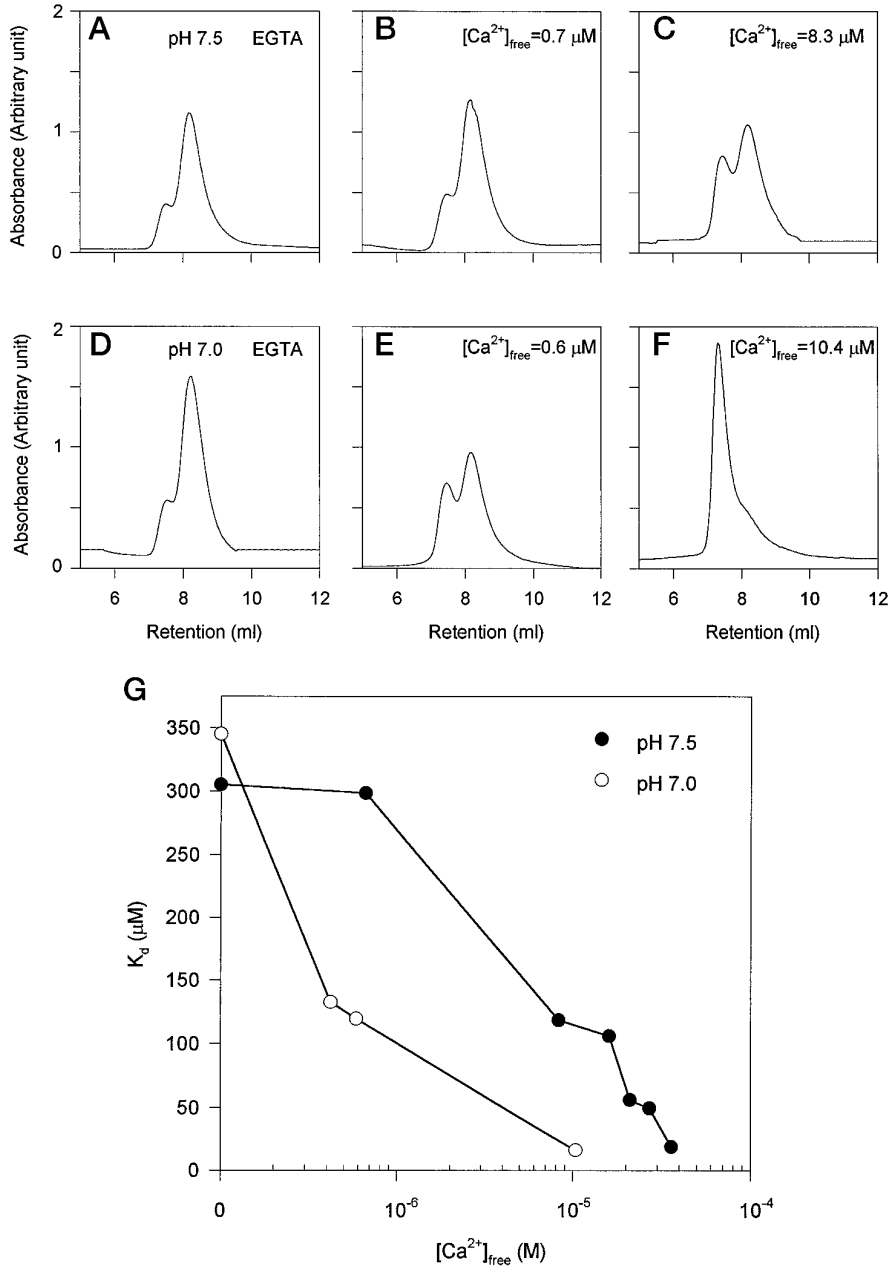

FIG. 5. **Effects of Ca^{2+} and pH on the binding of gelsolin to PIP_2, as determined by small zone gel filtration.** 2.3 μM gelsolin was incubated with 56.7 μM PIP_2 in a pH 7.5 or 7.0 buffer containing 0.4 μM EGTA and increasing amounts of $CaCl_2$. The free Ca^{2+} concentration was determined as described under "Experimental Procedures." *A–F*, gelsolin elution profiles. *A–C*, pH 7.5; *D–F*, pH 7.0. The K_d values at pH 7.5, from *left* to *right*, are 323.2, 298.6, and 118.6 μM, respectively. K_d values at pH 7.0, from *left* to *right*, are 345.2, 119.7, and 16.2 μM, respectively. *G*, plot of K_d *versus* Ca^{2+} concentration, at two different pH values.

TABLE II
Binding of gelsolin to PIP$_2$

	K_d (μM)					
	Fluorescence[a]				Gel filtration	
	EGTA	Ca^{2+}	p[b]	h[c]	EGTA	Ca^{2+}
Gelsolin (S1–6)			(3.0)		305.4 ± 20.2 (n = 7)[d]	40.2 ± 10.7 (n = 3)
NH_2-half (S1–3)	1.3 ± 0.3	2.9 ± 0.7	3.4	1.0 ± 0.03	4.3 ± 1.1 (n = 7)	7.4 ± 0.7 (n = 4)
S1	4.2 ± 2.3		1.6	0.9 ± 0.2		
S2–3	1.0 ± 0.2	2.9 ± 0.9	2.1	1.0 ± 0.1		
COOH-half (S4–6)	9.7 ± 0.4	20.0 ± 1.2		0.9 ± 0.2	52.0 ± 3.0 (n = 3)	137.7 ± 4.2 (n = 3)

[a] Fluorescence titration results were mean ± S.E. for three independent experiments.
[b] p, stoichiometry of binding (mol of PIP_2/mol of protein), average of two determinations. Stoichiometry for gelsolin is assumed to be 3.
[c] h, Hill coefficient.
[d] n, number of gel filtration experiments.

PIP_2 with a K_d of 4.2 μM in EGTA, while S2–3 bound 2.1 μmol of PIP_2 with a K_d of 1.0 and 2.9 μM in EGTA and Ca^{2+}, respectively (Table II).

The gelsolin COOH-terminal half bound PIP_2 with much lower affinity (approximately 7-fold higher K_d by fluorescence measurements) than the NH_2-terminal half (Table II). It is therefore probably not involved in PIP_2 binding *per se*. As with the NH_2-terminal half, binding to the COOH-terminal half was reduced in Ca^{2+} (Fig. 7*C*). This is in sharp contrast to the large Ca^{2+}-enhancement of PIP_2 binding to full-length gelsolin. The

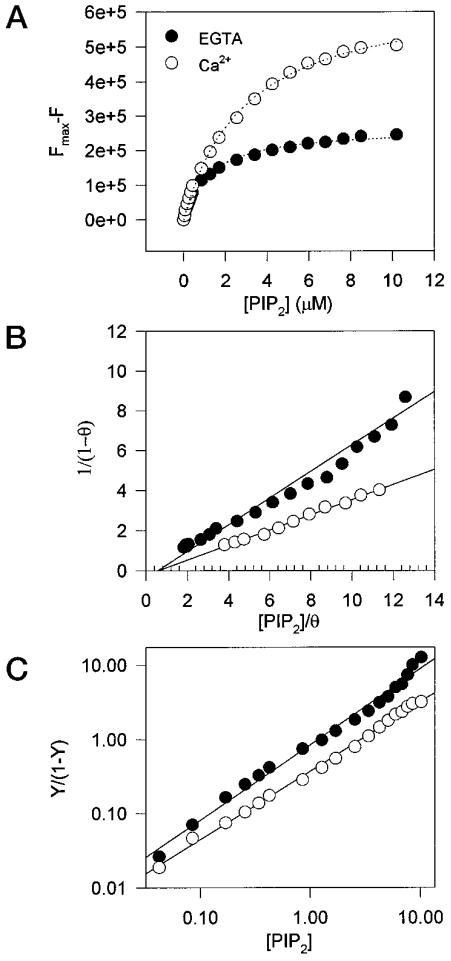

FIG. 6. **Effects of Ca^{2+} on the binding of the gelsolin NH_2-terminal half to PIP_2, as determined by fluorescence titration.** *A*, NH_2-terminal half (0.2 μM), with and without 36 μM Ca^{2+} in buffer containing 0.4 mM EGTA. PIP_2 concentration ranged from 0.04 to 10.2 μM. *B*, binding curves as described by Stinson and Holbrook (41). K_a is derived from the slope, and *p*, the stoichiometry of binding, is derived from the intercept divided by the protein concentration. *C*, Hill plot of binding in the presence of EGTA.

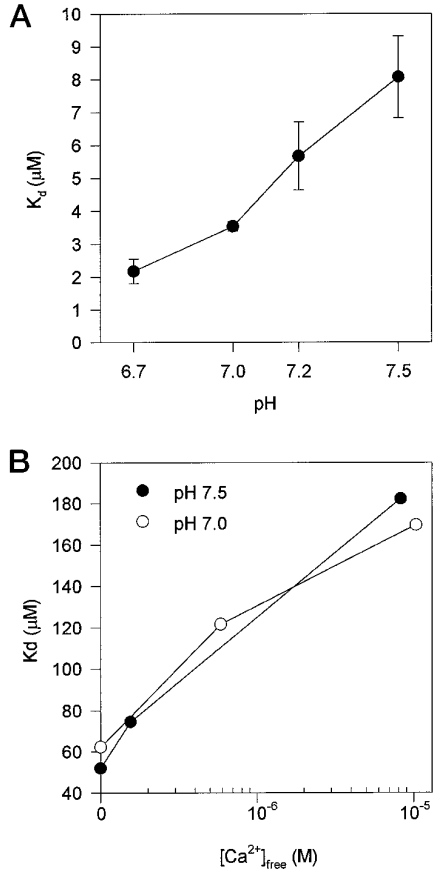

FIG. 7. **Effects of pH on the binding of gelsolin NH_2- and COOH-terminal halves to PIP_2, as determined by gel filtration.** *A*, gelsolin NH_2-terminal half (4 μM) binding to 11.3 and 22.7 μM PIP_2 as a function of pH. Values shown are the mean of two determinations, and the range is indicated. *B*, COOH-terminal half (5.8 μM) binding to 22.7 μM PIP_2 as a function of pH and Ca^{2+}.

opposite effects of Ca^{2+} on full-length and half-length gelsolins therefore cannot simply be due to nonspecific lipid aggregation. The pronounced enhancement of PIP_2 binding to full-length gelsolin most likely reflects a Ca^{2+}-dependent exposure of the NH_2-terminal half PIP_2 binding sites through a change in the COOH-terminal half. This conclusion is based on the observation that neither the NH_2- nor COOH-terminal halves are activated by Ca^{2+} to bind PIP_2, and only the COOH-terminal half is known to undergo Ca^{2+}-induced conformational change (51).

Gelsolin NH_2-terminal half binding to PIP_2 was enhanced by lowering pH. The K_d dropped from 8.2 to 3.4 μM between pH 7.5 and 7.0 in the presence of EGTA (Fig. 7*A*). In contrast, the gelsolin COOH-terminal half was not affected by pH (Fig. 7*B*).

DISCUSSION

Actin polymerization in response to agonist activation is frequently associated with a rise in cytosolic Ca^{2+}, changes in PIP_2 content, and intracellular pH. There is also compelling evidence that gelsolin, which severs and caps actin filaments in response to changes in Ca^{2+} and PIP_2 concentration and pH, is involved in actin remodeling (17, 52–54). In this paper, we show that gelsolin and CapG binding to PIP_2 is affected by physiologically relevant changes in Ca^{2+} and pH. The effects are not due to alterations in PIP_2 structure *per se* but reflect changes in the proteins. This is the first report that PIP_2 binding to any protein is directly modulated by signals generated during agonist stimulation and has implications for divergent PIP_2-dependent processes beyond a direct effect on the cytoskeleton.

The finding that gelsolin binding to PIP_2 is promoted by Ca^{2+} is consistent with the current model for how gelsolin is activated by Ca^{2+} to bind actin (48, 51). Our deletion studies suggest that the extreme COOH terminus of gelsolin is critical to the inhibition of the NH_2-terminal actin binding sites, because gelsolin lacking the COOH-terminal 23 residues no longer requires Ca^{2+} to bind actin (56). We do not know at present whether actin binding and PIP_2 binding are regulated identically. This question can now be addressed, because the actin and PIP_2-binding sites of gelsolin have been mapped (33, 50, 56–58) and the crystal structures of gelsolin S1 complexed with actin (57) and full-length gelsolin in EGTA[2] have been solved recently.

Less is known about how pH affects gelsolin conformation. Selve and Wegner (59) first reported that pH 6 increases the rate of gelsolin binding to actin in the presence of Ca^{2+}. Lamb *et al.* (26) subsequently showed that the Ca^{2+} requirement for gelsolin severing is reduced at pH 6.5 and abolished at pH below 6.0. pH 5 induces gelsolin unfolding, as determined by dynamic light scattering (26). We find that a less extreme pH drop potentiates Ca^{2+} activation of PIP_2 binding to full-length

[2] Burtnick, L. D., Koepf, E. K., Grimes, J., Jones, E. Y., Stuart, D. I., McLaughlin, P. J., and Robinson, R. C. (1997) *Cell*, in press.

gelsolin. Acidic pH increases the NH_2-terminal half binding to PIP_2 even without Ca^{2+} but has no effect on COOH-terminal half binding. Therefore, mild acidification probably promotes PIP_2 binding by directly altering the NH_2-terminal PIP_2 binding sites.

The significance of an increase in PIP_2 affinity described here depends on the PIP_2 concentration in the plasma membrane. This is difficult to estimate precisely because PIP_2 may be partitioned and sequestered. One estimate, based on PIP_2 accounting for 1% of plasma membrane lipid, suggests that the PIP_2 concentration in the plasma membrane of a spherical cell with a radius of 10 μm is 10 μM (44). In platelets, the PIP_2 concentration is estimated to be about 300 μM when averaged over the entire cell volume (internal and plasma membranes) (60), and PIP_2 concentration decreases by 30% following stimulation (16). Cytosolic [Ca^{2+}] rises during agonist stimulation, and the 4–8-fold increase in CapG and gelsolin binding affinity described here is sufficiently large to promote their increased association with the plasma membrane despite a modest decrease in membrane PIP_2. The magnitude of the increase depends on the PIP_2 concentration before and after stimulation. Immunogold labeling studies show that 4 and 6.5% of gelsolin is associated with the plasma membrane in resting and activated platelets, respectively (42). This represents a 63% increase in membrane association after stimulation. Our finding that Ca^{2+} increases PIP_2 binding affinity can explain how PIP_2 uncaps gelsolin and CapG even as the plasma membrane PIP_2 content decreases following agonist stimulation.

Since only a handful of the currently identified PIP_2-binding proteins are Ca^{2+}- and pH-sensitive, our finding is consistent with a selective regulation of the gelsolin family. Nevertheless, increased gelsolin and CapG binding will impact multiple PIP_2-dependent processes by altering PIP_2 availability to other binding proteins, especially when PIP_2 concentration is decreased during agonist stimulation. Some actin-binding proteins are inhibited by PIP_2 (profilin, cofilin, capping protein), while others are activated (α-actinin and vinculin). Gelsolin and CapG can therefore exert positive as well as negative effects indirectly by controlling PIP_2. We postulate that as the cytosolic [Ca^{2+}] rises during stimulation, gelsolin severs filaments and PIP_2 dissociates it from the filament end. Increased gelsolin binding to PIP_2 displaces capping protein and profilin, neither of which are Ca^{2+}-sensitive, from the plasma membrane. Profilin catalyzes polymerization (16), and the reaction is terminated by capping protein-mediated filament capping (55). Multiple rounds of severing, uncapping, and facilitated actin addition at the barbed ends fuel explosive amplification of filament growth observed during lamellipodial extension and membrane ruffling.

Our findings also have implications beyond a direct effect on the cytoskeleton. Many important signaling proteins are regulated by PIP_2 as well. It is significant that several pleckstrin homology proteins (reviewed in Ref. 2) bind PIP_2 with similar affinity as the gelsolin family. For example, the K_d values of β-adrenergic receptor kinase type 1, pleckstrin, dynamin, and phospholipase C_δ are 50, 50, 4, and 1 μM, respectively. Therefore, gelsolin and CapG can potentially compete with them for PIP_2, particularly when the [Ca^{2+}] rises and PIP_2 level drops during agonist stimulation. This possibility is supported by *in vitro* and *in vivo* experiments. *In vitro*, gelsolin stimulates and inhibits inositol-specific phospholipase C isozymes in a biphasic manner (29).[3] Gelsolin stimulates phosphoinositide 3-OH-kinase (31), although we find that gelsolin and CapG also inhibit it.[4] Gelsolin activates phospholipase D (30) in a PIP_2-dependent manner. Modest overexpression of CapG (28) or gelsolin has profound effects on phospholipase Cβ and phospholipase Cγ activated through two distinct receptor-mediated pathways.[3]

In conclusion, these observations show that gelsolin and CapG binding to PIP_2 is selectively regulated by second messengers. This regulation provides an additional level of control above that of a bulk change in PIP_2 content. Differential modulation and cross-talk between the PIP_2-binding proteins allow control to be exerted at multiple points in the signaling cascade.

Acknowledgments—We thank Drs. J. Albanesi, D. Hilgemann, and P. Thomas for helpful discussions and L. Segura for excellent technical assistance.

REFERENCES

1. De Camilli, P., Emr, S. D., McPherson, P. S., and Novick, P. (1996) *Science* **271,** 1533–1539
2. Shaw, G. (1996) *BioEssays* **18,** 35–46
3. Janmey, P. A. (1994) *Annu. Rev. Physiol.* 169–191
4. Schafer, D. A., and Cooper, J. A. (1995) *Annu. Rev. Cell Dev. Biol.* **11,** 497–518
5. Janmey, P. A., and Stossel, T. P. (1987) *Nature* **325,** 362–364
6. Yu, F.-X., Johnston, P. A., Sudhof, T. C., and Yin, H. L. (1990) *Science* **250,** 1413–1415
7. Schafer, D. A., Jennings, P. B., and Cooper, J. A. (1996) *J. Cell. Biol.* **135,** 169–179
8. Lassing, I., and Lindberg, U. (1985) *Nature* **314,** 604–606
9. Yonezawa, N., Nishida, E., Iida, K., Yahara, I., and Sakai, H. (1990) *J. Biol. Chem.* **265,** 8382–8386
10. Fukami, K., Furuhashi, K., Inagaki, M., Endo, T., Hatano, S., and Takenawa, T. (1992) *Nature* **359,** 150–152
11. Gilmore, A. P., and Burridge, K. (1996) *Nature* **381,** 531–535
12. Sun, H.-Q., Kwiatkowska, K., and Yin, H. L. (1995) *Curr. Opin. Cell Biol.* **7,** 102–110
13. Hall, A. (1994) *Annu. Rev. Cell Biol.* **10,** 31–54
14. Tolias, K. F., Cantley, L. C., and Carpenter, C. L. (1995) *J. Biol. Chem.* **270,** 17656–17659
15. Ren, X.-D., Bokoch, G. M., Traynor-Kaplan, A., Jenkins, G. H., Anderson, R. A., and Schwartz, M. A. (1996) *Mol. Biol. Cell* **7,** 435–442
16. Hartwig, J. H., Bokoch, G. M., Carpenter, C. L., Janmey, P. A., Taylor, L. A., Toker, A., and Stossel, T. P. (1995) *Cell* **82,** 643–653
17. Chen, P., Murphy-Ullrich, J. E., and Wells, A. (1996) *J. Cell. Biol.* **134,** 689–698
18. Apgar, J. R. (1995) *Mol. Biol. Cell* **6,** 97–108
19. Dadabay, C. Y., Patton, E., Cooper, J. A., and Pike, L. J. (1991) *J. Cell Biol.* **112,** 1151–1156
20. Bengtsson, T., Rundquist, I., Stendahl, O., Wymann, M. P., and Andersson, T. (1988) *J. Biol. Chem.* **263,** 17385–17389
21. Eberle, M., Traynor-Kaplan, A. E., Sklar, L. A., and Norgauer, J. (1990) *J. Biol. Chem.* **265,** 16725–16728
22. Pike, L. J., and Casey, L. (1996) *J. Biol. Chem.* **271,** 26453–26456
23. Hope, H. R., and Pike, L. J. (1996) *Mol. Biol. Cell* **7,** 843–851
24. Glaser, M., Wanaski, S., Buser, C. A., Boguslavsky, V., Rashidzada, W., Morris, A., Rebecchi, M., Scarlata, S. F., Runnels, L. W., Prestwich, G. D., Chen, J., Aderem, A., Ahn, J., and McLaughlin, S. (1996) *J. Biol. Chem.* **271,** 26187–26193
25. Yin, H. L., Zaner, K. S., and Stossel, T. P. (1980) *J. Biol. Chem.* **255,** 9494–9500
26. Lamb, J. A., Allen, P. G., Tuan, B. Y., and Janmey, P. A. (1993) *J. Biol. Chem.* **268,** 8999–9004
27. Young, C. L., Feierstein, A., and Southwick, F. S. (1994) *J. Biol. Chem.* **269,** 13997–14002
28. Sun, H.-Q., Kwiatkowska, K., Wooten, D. C., and Yin, H. L. (1995) *J. Cell Biol.* **129,** 147–156
29. Banno, Y., Nakashima, T., Kumada, T., Ebisawa, K., Nonomura, Y., and Nozawa, Y. (1992) *J. Biol. Chem.* **267,** 6488–6494
30. Steed, P. M., Nagar, S., and Wennogle, L. P. (1996) *Biochemistry* **35,** 5229–5237
31. Singh, S. S., Chauhan, A., Murakami, N., and Chauhan, V. P. (1996) *Biochemistry* **96,** 16544–16549
32. Kwiatkowski, D. P., Stossel, T. P., Orkin, S. H., Mole, J. E., Colten, H. R., and Yin, H. L. (1986) *Nature* **323,** 455–458
33. Yu, F.-X., Sun, H.-Q., Janmey, P. A., and Yin, H. L. (1992) *J. Biol. Chem.* **267,** 14616–14621
34. Yu, F.-X., Zhou, D., and Yin, H. L. (1991) *J. Biol. Chem.* **266,** 19269–19275
35. Sun, H.-Q., Wooten, D. C., Janmey, P. A., and Yin, H. L. (1994) *J. Biol. Chem.* **269,** 9473–9479
36. Bradford, M. M. (1976) *Annu. Rev. Biochem.* **72,** 248–254
37. Machesky, L. M., Goldschmidt-Clermont, P. J., and Pollard, T. D. (1990) *Cell Regul.* **1,** 937–950
38. Goldschmidt-Clermont, P. J., Machesky, L. M., Baldassare, J. J., and Pollard, T. D. (1990) *Science* **247,** 1575–1578

[3] Sun, H.-Q., Lin, K.-M., and Yin, H. L. (1997) *J. Cell Biol.*, in press.

[4] P.-J. Lu, A.-L. Hsu, D.-S. Wang, H. Yan, H. L. Yin, and C.-S., Chen, manuscript in preparation.

39. Hummel, J. P., and Dreyer, W. J. (1962) *Biochim. Biophys. Acta* **63,** 530–532
40. Ward, L. D. (1985) in *Methods Enzymol.* (Ward, L. D., ed) pp. 400–414, Academic Press, Inc., New York
41. Stinson, R. A., and Holbrook, J. J. (1997) *Biochem. J.* **131,** 719–728
42. Hartwig, J. H., Chambers, K. A., and Stossel, T. P. (1989) *J. Cell Biol.* **108,** 467–479
43. Lu, P., Shieh, W., Rhee, S. G., Yin, H. L., and Chen, C. (1996) *Biochemistry* **35,** 14027–14034
44. Garcia, P., Gupta, R., Shah, S., Morris, A. J., Rudge, S. A., Scarlata, S., Petrova, V., McLaughlin, S., and Rebecchi, M. J. (1995) *Biochemistry* **34,** 16228–16234
45. Zheng, J., Cahill, S. M., Lemmon, M. A., Fushman, D., Schlessinger, J., and Cowburn, D. (1996) *J. Mol. Biol.* **22,** 14–21
46. Janmey, P. A., Iida, K., Yin, H. L., and Stossel, T. P. (1987) *J. Biol. Chem.* **262,** 12228–12236
47. van Paridon, P. A., de Kruijff, B., Ouwerkerk, R., and Wirtz, K. W. (1986) *Biochim. Biophys. Acta* **877,** 216–219
48. Chaponnier, C., Janmey, P. A., and Yin, H. L. (1986) *J. Cell Biol.* **103,** 1473–1481
49. Yin, H. L., Iida, K., and Janmey, P. A. (1988) *J. Cell Biol.* **106,** 805–812
50. Janmey, P. A., Lamb, J., Allen, P. G., and Matsudaira, P. T. (1992) *J. Biol. Chem.* **267,** 11818–11823
51. Kwiatkowski, D., Janmey, P. A., Mole, J. E., and Yin, H. L. (1985) *J. Biol. Chem.* **260,** 15232–15238
52. Cunningham, C. C., Stossel, T. P., and Kwiatkowski, D. J. (1991) *Science* **251,** 1233–1236
53. Witke, W., Sharpe, A. H., Hartwig, J. H., Azuma, T., Stossel, T. P., and Kwiatkowski, D. J. (1995) *Cell* **81,** 41–51
54. Arora, P. D., and McCulloch, C. A. G. (1996) *J. Biol. Chem.* **271,** 20516–20523
55. Barkalow, K., Witke, W., Kwiatkowski, D. J., and Hartwig, J. H. (1996) *J. Cell Biol.* **96,** 389–399
56. Kwiatkowski, D., Janmey, P. A., and Yin, H. L. (1989) *J. Cell Biol.* **108,** 1717–1726
57. McLaughlin, P. J., Gooch, J. T., Mannherz, H.-G., and Weeds, A. G. A. (1993) *Nature* **364,** 685–692
58. Van Troys, M., Dewitte, D., Goethals, M., Vandekerckhove, J., and Ampe, C. (1996) *FEBS Lett.* **96,** 191–193
59. Selve, N., and Wegner, A. (1987) *Eur. J. Biochem.* **168,** 111–115
60. Rittenhouse, S. E., and Sasson, J. P. (1985) *J. Biol. Chem.* **260,** 8657–8660